

A Model for Filler–Matrix Debonding in Glass-Bead-Filled Viscoelastic Polymers

A. MEDDAD, B. FISA

Centre de Recherche Appliqué sur les Polymères (CRASP), École Polytechnique de Montréal, Montréal, Québec H3C 3A7, Canada

Received 13 June 1996; accepted 14 February 1997

ABSTRACT: This article deals with the stress–strain behavior of two viscoelastic polymers, polypropylene and polyamide 6, filled with rigid particles in the range of axial strain of 0 to 8%. These materials, when subjected to a constant strain rate test lose stiffness via two mechanisms: filler–matrix debonding and the viscoelastic softening of the matrix. A model that combines the concepts of damage mechanics and the time dependence of the interfacial strength is described and compared to the experimental results of polypropylene and polyamide 6 filled with up to 50 vol % of untreated and silane-treated glass beads. The matrix behavior is described in terms of an empirical equation selected to fit the stress–strain behavior of neat polymers in the range of strain rates between 0.12 and 0.5% s⁻¹ and strains between 0 and 8%. The stiffness of the damaged, partially debonded composite is calculated using the Kerner–Lewis equation assuming that debonded particles do not bear any load. The model is able to generate stress–strain curves that are in good agreement with the experimental data. The void volume attributable to debonding calculated using the model is much smaller than the experimental total determined void volume (which is a sum of several deformation mechanisms). © 1997 John Wiley & Sons, Inc. *J Appl Polym Sci* **65**: 2013–2024, 1997

Key words: filler; polymer; debonding; damage; stress–strain behavior

INTRODUCTION

In the previous article¹ we discussed the contribution of the filler–matrix debonding to the results of the constant strain rate tensile test for the case when the matrix is viscoelastic. Two methods of identification of the onset of debonding were examined: the gradual loss of stiffness during the test, and the tensile dilatometry. It was concluded that although the tensile dilatometry appears more straightforward, its results are difficult to interpret because the volume change due to debonding is only a small part of the overall volume change recorded during the test. The loss of stiffness during the tensile test expressed, for example, as a ratio of the

secant moduli of the composite and of the matrix offers a simple method to detect and follow the debonding process in filled plastics and possibly in other multiphase materials.

In this work we analyze the debonding process in polypropylene and polyamide 6 filled with glass beads in terms of a model that uses concepts of damage mechanics and that takes into account the viscoelastic nature of the matrix polymers. Several approaches were proposed to describe the experimental data in materials damaged by the debonding process. One of the more simple methods consists in the direct application of the damage mechanics.² The debonding-induced damage is quantified with the help of the damage parameter D defined as follows:

$$D = 1 - \frac{\bar{E}}{E_{0c}} \quad (1)$$

Correspondence to: A. Meddad.

© 1997 John Wiley & Sons, Inc. CCC 0021-8995/97/102013-12

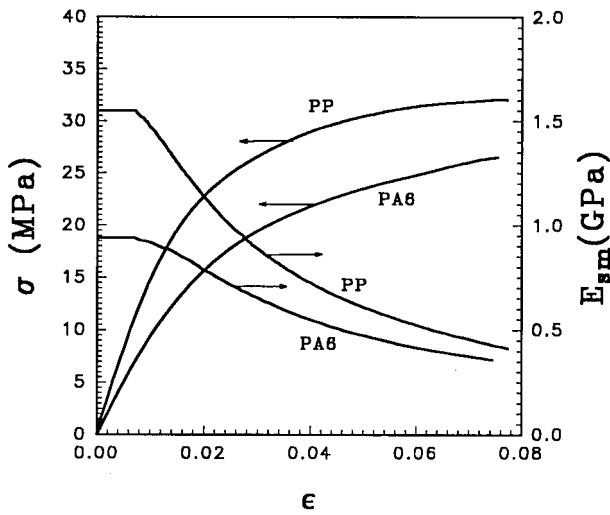


Figure 1 Stress σ versus ϵ strain and E_{sm} versus ϵ curves of neat PP and PA6.

where \bar{E} represents the modulus of the damaged (i.e., partially debonded) material while E_{oc} is the initial modulus of the undamaged composite. Newaz and Walsh³ used this concept to follow the debonding in sand and ash-filled epoxy resins. Because these materials, neat matrix, and composites are inherently elastic, any deviation from linear elasticity can be safely attributed to strain-induced damage (of which filler/matrix debonding is considered predominant, particularly in the low strain range). Using the “load–unload” tensile test, Newaz and Walsh have shown that the damage parameter D can be related to the debonding process. However, the physical significance of the results is not entirely satisfactory, principally because this approach fails to take into account the fact that the loss of stiffness cannot be attributed exclusively to the reduction of the effective load-bearing section. In addition to this, as the debonding progresses, only one, the more rigid phase, is being excluded from the load bearing and the effective filler concentration in the remaining material is reduced.

The model developed by Anderson and Farris,^{4,5} which was applied to a glass-bead-filled polyurethane elastomer, calculates the nonlinear stress–strain behavior of the filled polymer undergoing debonding using an energy balance based on the first law of thermodynamics. This model has been used to predict the loss of stiffness, assuming separately either a reduction of the effective filler concentration or an addition of voids, both resulting from debonding. This model has been recently applied to high-density polyeth-

ylene filled with glass beads.⁶ The predicted stress–strain behavior deviates from the experimental results, particularly after the elastic stage. This was attributed to the uncertain value of adhesion energy term in the equation governing the debonding process.

Recently, a mathematical model developed from the tensile stress–strain and from the volume strain data has been proposed by Zezin.⁷ It describes the damage accumulation in terms of debonded filler fraction. Other studies published recently present debonding models without comparing them to the experimental results. For example, the theory developed by Zhao and Weng⁸ to describe the debonding process in a ductile elastic composite containing aligned oblate inclusions, uses a statistical function to model the breakage of filler/matrix bonds. The constitutive model developed by Ravichandran and Liu⁹ is used to illustrate the behavior of a soft, nearly incompressible elastic matrix filled with rigid particles. It assumes that the composite behavior, in the absence of any damage, is linear elastic. The model considers the debonding-induced damage as an isotropic function, depending on an internal variable.

In summary, the simple methods do not yield satisfactory results because they do not take into account one or more of the critical features of the composite behavior. Moreover, the more general methods for mathematical description of fully or partially bonded composites are very awkward because of the filler agglomeration, thermal

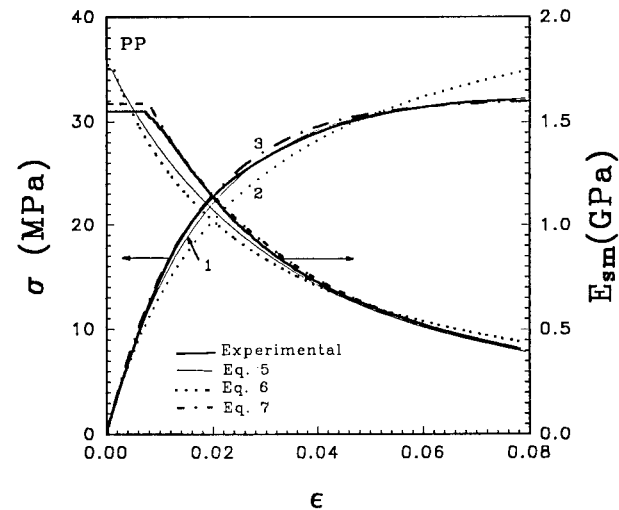


Figure 2 Stress–strain and secant modulus–strain curves of neat PP. (1) Maxwell model [eq. (6)]; (2) Menges model [eq. (7)]; (3) model described by eq. (8). Experimental curves are also shown (—).

Table I Material Constants for PP and PA6

	Maxwell's Model [Eq. (6)]	Menges Model [Eq. (7)]	Eq. (8)
PP	$E_{0m} = 1.75 \cdot 10^9$ Pa $t_r = 2.23$ s	$E_{0m} = 1.75 \cdot 10^9$ Pa $D_m = 40.47$	$E_{0m} = 1.58 \cdot 10^9$ Pa $a = 0.00018$ s ⁻¹ $b = -55.25$ Pa ⁻¹ $c = 4.22 \cdot 10^{-11}$ Pa ⁻¹ s ⁻¹ $d = -0.00018$ s ⁻¹
PA6	$E_{0m} = 1.1 \cdot 10^9$ Pa $t_r = 3.12$ s	$E_{0m} = 1.1 \cdot 10^9$ Pa $D_m = 25.50$	$E_{0m} = 0.98 \cdot 10^9$ Pa $a = 0.00019$ s ⁻¹ $b = -56.58$ Pa ⁻¹ $c = 4.86 \cdot 10^{-11}$ Pa ⁻¹ s ⁻¹ $d = -0.00019$ s ⁻¹

The correlation factors of Maxwell model is equal to 0.85 for PP and 0.87 for PA6, of Menges model is equal to 0.72 for PP and 0.64 for PA6, and of eq. (8) is equal to 0.94 for PP and 0.93 for PA6.

stresses, stress concentration, and innumerable other material heterogeneities that cannot be fully and accurately described.

A satisfactory model describing the stress–strain behavior in a viscoelastic material filled with rigid particles that become progressively separated from the matrix should have following features: (1) a realistic description of the matrix behavior as a function of stress, strain, and time; (2) ability to take into account the change of the composition of the load-bearing material as the more rigid filler particles become excluded and are replaced by effective voids; and (3) ability to describe the debonding process as a function of variables that can be readily measured (stress, strain, and time).

This article presents one model that was built to include these three features. The model has been used to calculate the stress–strain behavior of polypropylene and polyamide 6 containing various concentrations of untreated or silane-treated glass beads. Good agreement between the calculated and experimentally determined results was achieved. All the experimental details concerning the materials used, sample preparation, and mechanical testing can be found in the previous article.¹

MODEL FOR MATRIX BEHAVIOR

In the previous article we have shown that in the range of axial strains studied (0 to 8%), the curve of neat polypropylene (PP) could be characterized by three parts (Fig. 1): (1) a linear elastic part up to $\epsilon = 0.75\%$ with a constant secant modulus

$E_{sm} = 1.57$ GPa; (2) a nonlinear zone characterized by a gradual rapid decrease of the secant modulus; (3) at $\epsilon = 7.5\%$, the stress–strain curve reaches a maximum which, by convention, corresponds to yield; and (4) beyond $\epsilon 7.5\%$ the nominal stress remains approximately constant up to strain of about 20%.

The behavior of neat polyamide 6 is similar to that of polypropylene (Fig. 1). The secant modulus E_{sm} assumes constant value of 0.92 GPa up to the axial strain $\epsilon = 0.73\%$. However, in the range of strains studied ($\epsilon < 8\%$), the polyamide 6 stress–strain curve has not reached a maximum and the nominal stress continues to rise, albeit at a slow rate.

There is a vast body of literature on the mechanical behavior of viscoelastic materials. We have examined the suitability of several simple models available for the description of the stress–strain behavior of polypropylene and polyamide 6 in the range of strains and strain rates used (0–8% and 0.12–0.5% s⁻¹).

For a viscoelastic material, the strain rate $\dot{\epsilon}$ imposed during a constant strain rate test can be decomposed into “elastic” and “inelastic” additive components:

$$\dot{\epsilon} = \dot{\epsilon}_e + \dot{\epsilon}_n = \text{const.} \quad (2)$$

where $\dot{\epsilon}_e$ and $\dot{\epsilon}_n$ represent the elastic and inelastic strain rates, respectively.

Then the following elastic strain rate $\dot{\epsilon}_e$ can be defined as

$$\dot{\epsilon}_e = \frac{\dot{\sigma}}{E_{0m}} \quad (3)$$

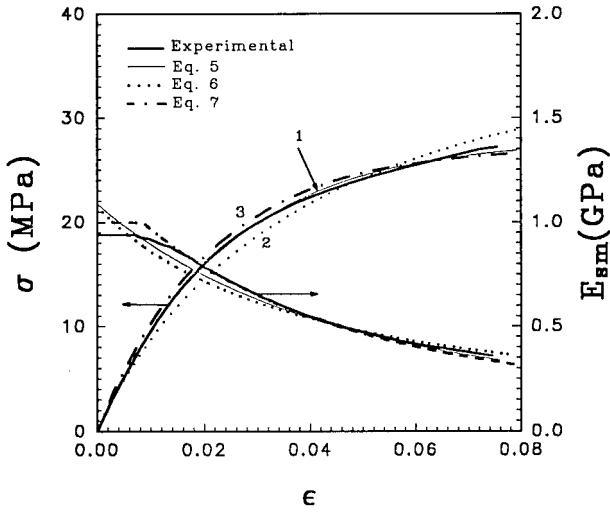


Figure 3 Stress–strain and secant modulus–strain curves of neat PA6. (1) Maxwell model [eq. (6)]; (2) Menges model [eq. (7)]; (3) Model described by eq. (8). Experimental curves are also shown (—).

where E_{0m} is the initial modulus and $\dot{\sigma}$ represents the rate of stress change.

The inelastic strain rate $\dot{\epsilon}_n$ as a function of applied stress σ and time t is

$$\dot{\epsilon}_n = f(\sigma, t) \quad (4)$$

One of the simplest viscoelastic materials, the Maxwell model, is defined by two constants, the initial modulus E_{0m} and a single relaxation time t_r . In the Maxwell body undergoing a constant strain rate test, the inelastic strain rate $\dot{\epsilon}_n$ is

$$\dot{\epsilon}_n = \sigma / E_{0m} t_r \quad (5)$$

The stress–strain curve is given by

$$\sigma = \dot{\epsilon} E_{0m} t_r \left[1 - \exp\left(\frac{-\epsilon}{\dot{\epsilon} t_r}\right) \right] \quad (6)$$

Using eq. (6) and a curve-fitting method, appropriate values of E_{0m} and t_r can be found for each strain rate with a relatively good correlation factor (see, e.g., curve 1 for $\dot{\epsilon} = 0.122\% \text{ s}^{-1}$ (Fig. 2), where the correlation factor is equal to 0.85). It is clear, however, from the E_{sm} versus presentation that the Maxwell model, and for that matter any other linear viscoelastic model, cannot account for the initial constant stiffness zone ($0 < \epsilon < \epsilon_0$). The same deviation holds for one of the most widely used empirical models for the

stress–strain behavior of plastics solicited in the tensile mode, which was proposed by Menges and Schmaectenberg.¹⁰ For semicrystalline polymers at temperatures above the glass transition temperature, it has the following form:

$$\sigma = \frac{E_{0m}\epsilon}{1 + D_m\epsilon} \quad (7)$$

where the E_{0m} represents the initial modulus (at $\epsilon \rightarrow 0$) and D_m is a function of strain rate. The best correlation for $\dot{\epsilon} = 0.122\% \text{ s}^{-1}$ is also shown in Figure 2 (curve 2, where the correlation factor is equal to 0.72). In addition to the absence of the constant stiffness region, this model with the optimized constants D_m and E_{0m} does not reach the constant stress plateau, which we observe in polypropylene.

Having examined a number of other, more complex models we have finally adapted the following relation for the inelastic strain rate:

$$\dot{\epsilon}_n = a \exp(b\sigma) + c\sigma + d = \dot{\epsilon} - \frac{\dot{\sigma}}{E_{0m}} \quad (8)$$

Experimental stress–strain data collected at three testing speeds (0.0833, 0.166, and 0.33 mm s^{-1}), which correspond to strain rates of 0.12, 0.24, and 0.5% s^{-1} , were used to optimize the values of constants shown in Table I. It can be seen that a numerical integration of eq. (8) using the optimized constants yields stress–strain (σ vs. ϵ) and secant modulus–strain (E_{sm} vs. ϵ) (curves 3), which exhibit all important features of the experimental curves, namely constant stiffness at small

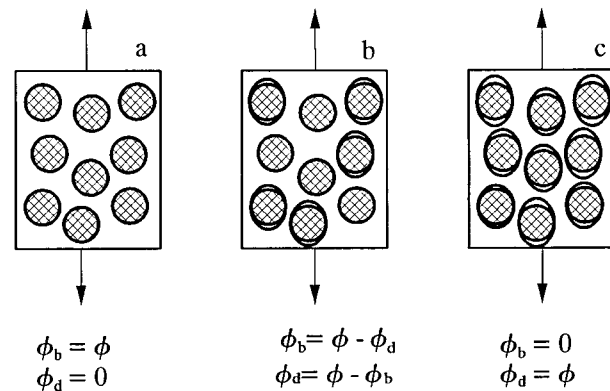


Figure 4 Schematic representation of a filled polymer subjected to uniaxial tension. (a) Well-bonded composite; (b) partially debonded composite; and (c) fully debonded composite.

Table II Parameters Used to Calculate the Initial Composite Mode Modulus E_{0c} from Eq. (11)

Parameters	PP	PA6
E_{0m} (GPa)	1.62	0.88
A_1	1.68	1.90
B_1	0.85	1.03
ψ	0.60	1.04

strains (Figs. 2 and 3, curve 3). This model [eq. (8)] was selected as adequate for the description of the matrix behavior.

Debonding Model

In the preceding article¹ we have shown that the small strain behavior of glass-bead-filled polypropylene was that of fully bonded composite, which for volume fractions of up to and including 0.2 obeys the Kerner–Lewis equation with constants calculated from the properties of the components. At higher filler loadings (up to $\phi = 0.5$) the Kerner–Lewis equation can be used as an interpolation formula with constants optimized to fit the experimentally determined E_{0c} versus ϕ dependence. In the fully debonded state the Kerner–Lewis equation can still be used to calculate the material stiffness considering each vacuole containing a debonded glass bead as a void. The material is considered to behave as a foam containing void volume fraction equal to ϕ .

The process that is modeled is illustrated in Figure 4. A composite material containing a volume fraction ϕ of filler is subjected to a constant strain rate test. The following is assumed: (1) Initially all filler particles are well bonded to the matrix (bonded filler volume fraction $\phi_b = \phi$ [Fig. 4(a)]. The material behavior can be described by the Kerner–Lewis equation with the constants listed in Table II (see below). (2) Upon straining, the filler particles become progressively debonded ($\phi_b = \phi - \phi_d$, ϕ_d being the debonded filler volume fraction). The debonded particles do not bear any load [Fig. 4(b)]. (3) The completely debonded composite $\phi_b = 0$, $\phi_d = \phi$ behaves as a foam containing volume fractions of voids equal to ϕ_d . Its behavior can also be described by the Kerner–Lewis equation [Fig. 4(c)]. (4) The debonding rate ($d\phi_d/dt$) depends on the applied stress and on the number of particles available for debonding ($\phi - \phi_d$).

During the constant strain rate tensile test ($d\epsilon/dt = \text{const}$), the measured stress σ follows the relation

$$\frac{d\sigma}{dt} = \frac{d(E_{sc} \cdot \epsilon)}{dt} = \epsilon \cdot \frac{dE_{sc}}{dt} + E_{sc} \cdot \frac{d\epsilon}{dt} \quad (9)$$

where E_{sc} is the secant modulus of the composite. The composite modulus (E_{sc}) decreases as the debonding progresses and as the accumulated inelastic strain of the matrix (ϵ_n) increases. The partially debonded composite containing a volume fraction ϕ of the filler (of which ϕ_d is debonded: $0 \leq \phi_d \leq \phi$) is considered to consist of three components: (1) matrix, which has the secant modulus E versus ϵ dependence shown in Figures 2 or 3, and which can be described by eq. (8) using parameters of Table I; (2) bonded filler [volume fraction ($\phi - \phi_d$)]; and (3) debonded filler—each vacuole containing a debonded filler particle behaves as a void.

The modulus of such hybrid material can be described by the Kerner–Lewis equation¹¹:

$$E_{sc} = E_{sm} \cdot E_1 \cdot E_2 \quad (10)$$

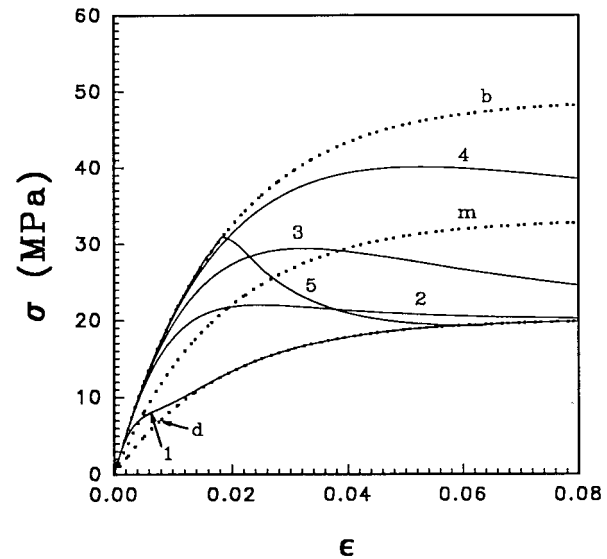


Figure 5 Stress–strain curves calculated using eqs. (9) and (14) (see text): (m) matrix; (b) fully bonded composite; (d) fully debonded composite. Curves 1–5 were calculated using the following values of constants K and B : (1) $K = 3.04 \cdot 10^{-2} \text{ MPa}^{-1} \text{ s}^{-1}$, $B = 0$; (2) $K = 2.03 \cdot 10^{-3} \text{ MPa}^{-1} \text{ s}^{-1}$, $B = 0$; (3) $K = 6.80 \cdot 10^{-4} \text{ MPa}^{-1} \text{ s}^{-1}$, $B = 0$; (4) $K = 1.2 \cdot 10^{-4} \text{ MPa}^{-1} \text{ s}^{-1}$, $B = 0$; (5) $K = 2.03 \cdot 10^{-14} \text{ MPa}^{-1} \text{ s}^{-1}$, $B = 1 \text{ MPa}^{-1}$.

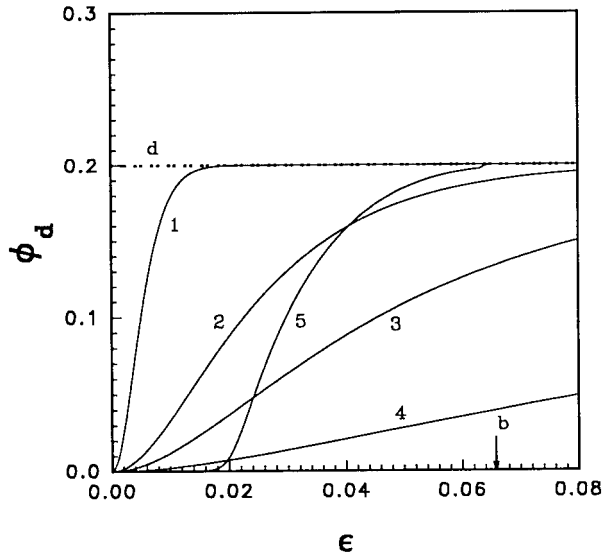


Figure 6 Debonded filler fraction ϕ_d calculated using eqs. (9) and (14) as a function of strain ϵ . The curves are numbered as in Figure 5.

where E_1 represents the relative modulus of the still bonded filled material:

$$E_1 = \frac{1 + A_1 \cdot B_1 \cdot (\phi - \phi_d)}{1 - B_1 \cdot \Psi \cdot (\phi - \phi_d)} \quad (11)$$

with constants A_1 , B_1 and Ψ determined by fitting the experimental small strain composite modulus E_{sc} versus filler volume fraction ϕ dependence. The modulus E_2 is the relative modulus of the foam with a void fraction equal to ϕ_d . E_2 is then given by

$$E_2 = \frac{1 - \phi_d}{1 - B_2 \cdot \Psi \cdot \phi_d} \quad (12)$$

with $B_2 = -1/A_1$. It is worth noting that the Kerner–Lewis equation and other expressions of this type have been successfully applied to hybrid materials¹² and to high-density foams.¹³

Considering the heterogeneous nature of materials under consideration it seems reasonable to adapt Bartenev's equation^{14,15} for time to failure, t_f , of a material subjected to an effective stress, $\bar{\sigma}$. This equation, originally developed for materials containing defects, is written here in a simplified form:

$$t_f = \frac{\exp(-B \cdot \bar{\sigma})}{K \cdot \bar{\sigma}} \quad (13)$$

The constants B and K depend on the temperature, the material molecular structure, and on the nature and number of defects. It should be noted that although this and other equations (e.g., Zhurkov–Bueche¹⁶) relating the time to failure to the applied stress have a theoretical basis, they are often considered as interpolation formulas of semiempirical nature—useful for mathematical expression of experimental data. Applying the Bartenev's concept to a filled material, we assume that the time to failure of the filler/matrix interface can be described by eq. (13). The probability of debonding is proportional to $1/t_f$. The debonding rate $d\phi_d/dt$ is then considered to be proportional to $K\bar{\sigma} \exp(B\bar{\sigma})$ (the constants K and B are related to the overall behavior of the filled material rather than only to that of the single particle/matrix interface, $\bar{\sigma}$ is the effective stress—see below) and to $(\phi - \phi_d)$.

$$\frac{d\phi_d}{dt} = (\phi - \phi_d) \cdot K \cdot \bar{\sigma} \exp(B \cdot \bar{\sigma}) \quad (14)$$

The effective stress $\bar{\sigma}$, which acts only on the matrix and on the still bonded filler, can be related to the measured stress σ (which is calculated using the entire sample cross section, including its debonded portion), using the strain equivalence principle.² A material containing a filler fraction $(\phi - \phi_d)$ but no voids will have a modulus E'_{sc} :

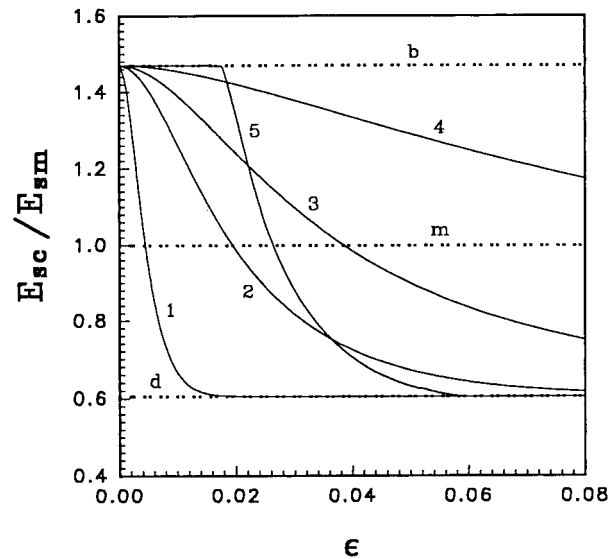


Figure 7 Relative modulus of composite (E_{sc}/E_{sm}) calculated using eq. (11) as a function of strain ϵ . The curves are numbered as in Figure 5.

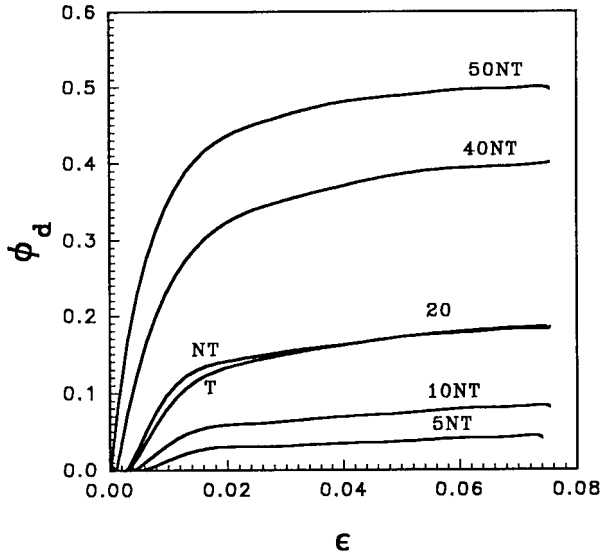


Figure 8 Volume fraction of debonded glass beads, ϕ_d , as a function of strain for PP filled with different glass concentration silane treated (T) and untreated (NT); calculated from experimental data using eq. (10).

$$E'_{sc} = E_{sm} \cdot E_1 \quad (15)$$

According to the strain equivalence principle,

$$\epsilon = \frac{\bar{\sigma}}{E'_{sc}} = \frac{\sigma}{E_{sc}} \quad (16)$$

This leads to

$$\bar{\sigma} = \frac{\sigma}{E_2} \quad (17)$$

Since

$$\frac{dE_{sc}}{dt} = \frac{dE_{sc}}{d\phi_d} \cdot \frac{d\phi_d}{dt} \quad (18)$$

a simultaneous solution of eqs. (9) and (14) can be obtained using known values of E_{sm} , $d\epsilon/dt$, and ϕ and using equations (10)–(12), (17), and (18).

Solution of eqs. (9) and (14) using the fourth-order Runge Kutta method yields the value of the secant modulus E_{sc} and of the debonded fraction ϕ_d . To determine the appropriate values of K and B , the calculated results are compared, with the help of the Marquardt–Levenberg algorithm, to the values of ϕ_d computed from the experimental stress–strain data using eq. (10).

The volume increase due to debonding, ζ_d , can also be calculated assuming, for example, that each void created by debonding of a spherical particle (diameter d) is an ellipsoid with its two shorter axes equal to d and its longer axis equal to $d \cdot [1 + (\epsilon - \epsilon_d)]$, where ϵ_d represents the strain at which the particle becomes debonded.⁷ It follows that

$$\zeta_d = \int_0^\epsilon \phi_d d\epsilon \quad (19)$$

Model Verifications

The debonding process modeled with the help of eqs. (9), (10), and (14) using the materials constants of neat and filled polypropylene (Tables I and II) and several arbitrarily selected values of K and B leads to stress strain curves shown in Figure 5. Two extreme cases are considered: (1) When the value of the exponential term constant B is set to 0, the debonding rate is proportional to the effective stress $\bar{\sigma}$. The measured stress σ versus ϵ function deviates from that of the fully bonded composite at a relatively low strain and moves to the completely debonded state over a broad range of strains (see also Fig. 6 for the cor-

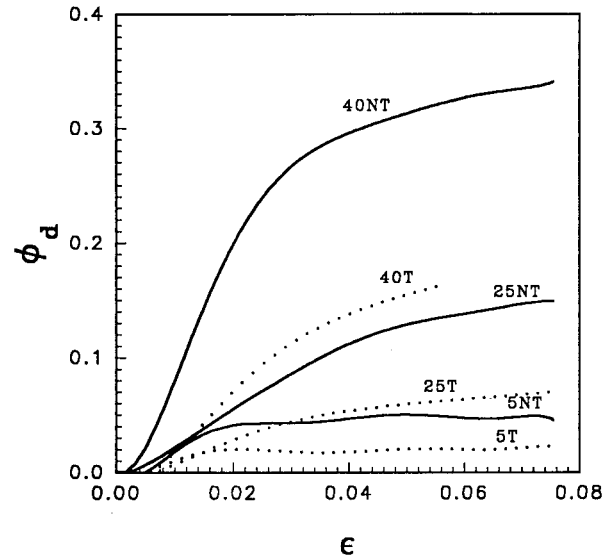


Figure 9 Volume fraction of debonded glass beads, ϕ_d , as a function of strain for PA6 filled with different glass concentration silane treated (T) and untreated (NT); calculated from experimental data using eq. (10).

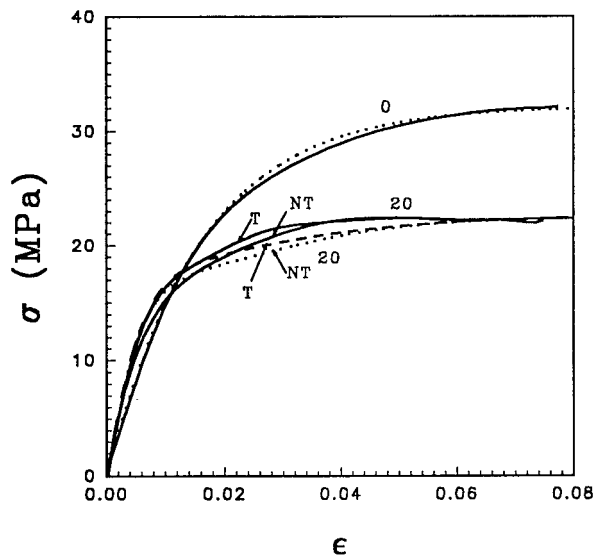


Figure 10 Stress-strain curves, predicted by the model and experimental (—) of 20 vol % filled PP; treated (T) and untreated (NT) glass.

responding ϕd vs. ϵ curves). With a high value of K (curve 1) the σ versus ϵ curve of the composite will cross that of the matrix when the matrix is still elastic and join that of the debonded composite at a strain well below the yield. The value of K used to draw curve 2 in Figure 5 was selected so that the debonding process would be complete in the range of strains studied experimentally (0 to 8%). In this case, the stress-strain curve reaches a maximum at about 1.5% strain when about a third of all filler particles have debonded. However, Figure 7 shows that the E_{sc}/E_{sm} curves do not have a low strain zone of constant stiffness that was observed in filled polypropylene and polyamide 6. (2) With a very high value of B , the debonding will occur at nearly constant effective stress ($\bar{\sigma}$). Curve 5 corresponds to this case. The stress-strain curve (σ vs. ϵ) follows that of a well-bonded composite until the onset of debonding (with the combination of K and B used at $\sigma = \bar{\sigma} = 32$ MPa). With the reduction of the load-bearing section the applied (measured) stress (σ) decreases (while $\bar{\sigma} = \text{const}$) until the fully debonded state is reached at $\sigma = 18$ MPa and $\epsilon = 6\%$. The apparent “yield” of the composite (maximum of the value σ vs. ϵ curve) corresponds to the onset of debonding rather than to the inherent yield of the matrix material. The corresponding ϕ_d versus and E_{sc}/E_{sm} versus curves are shown in Figures 6 and 7.

The shapes of these curves suggest that the

Bartenev-type equation can cover the range of situations likely to occur in glass-bead-filled viscoelastic materials. The extreme case of the debonding occurring at constant effective stress (curves 5, Figs. 5–7) will certainly not be found in real materials where the dispersed phase distribution is at best uniformly random, particles are of different sizes, local stress fluctuations are caused not only by the material inherent heterogeneities but also by residual stresses that vary throughout the thickness, and where the debonding will, therefore, occur over a broader range of stress and strain.

In the previous work we concluded that in glass-bead-filled polypropylene, in which the completely debonded state was reached, the Kerner–Lewis equation could be used to predict the stiffness of fully bonded and fully debonded material. It seems reasonable to assume that the same equation can be also used to describe the intermediate state of partial debonding.¹ Knowing the secant modulus of the composite, the ϕ_d versus ϵ dependence can be determined from eq. (10). Figure 8 shows the results for filled polypropylene. The ϕ_d versus curves, particularly those for lower glass concentrations ($\phi \leq 0.2$) exhibit two linear parts, the first one characterized by a rapid increase of ϕ_d at $>\epsilon_0$, the second plateau region as the material approaches the fully debonded state. The fact that ϕ_d values calculated for higher

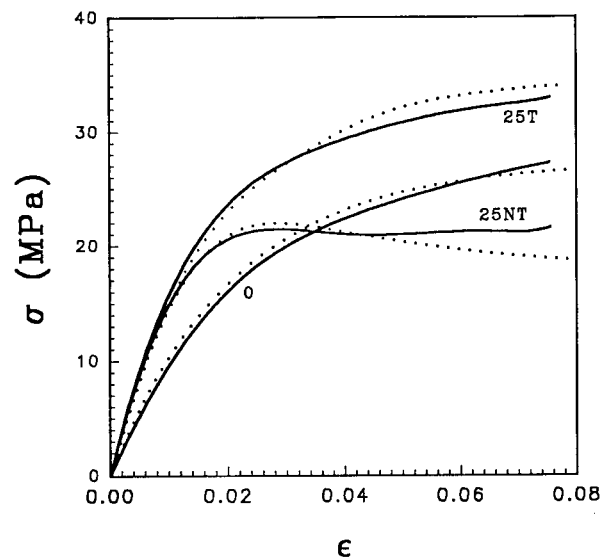


Figure 11 Stress-strain curves, predicted by the model and experimental (—) of 25 vol % of treated (T) and untreated (NT) filled PA6.

Table III *K* and *B* Values of Polypropylene (PP)/Glass Beads Composites

Glass Content (vol. %)	$K \times 10^2 \text{ MPa}^{-1} \text{ s}^{-1}$		$B \times 10^2 \text{ MPa}^{-1}$	
	NT	T	NT	T
10	9.0	7.0	0.07	0.02
20	4.30	3.10	0.11	0.09
40	2.10	1.47	1.92	1.45
50	1.65	1.15	4.80	4.2

NT, untreated glass beads; T, silane-treated glass beads.

strains do not always coincide with the exact glass content is caused by the differences between the measured stress borne by the composite at a given strain and that calculated from the stress borne by the matrix assuming complete debonding at the same strain [eq. (12)]. For example, at $\epsilon = 7.5\%$, the measured stress of polypropylene containing 20 vol % of untreated beads is 23 MPa. Using this value and the stress borne by the neat matrix at $\epsilon = 7.5\%$ to calculate the debonded filler fraction gives $\phi_d = 0.18$. Had the experimental value of stress at $\epsilon = 7.5\%$ been only 1 MPa lower, complete debonding ($\phi_d = 0.2$) would have been calculated. Applying the same procedure to filled polyamide 6 yields the results shown in Figure 9. As mentioned in the preceding article, in filled polyamide 6 the level of adhesion is higher even without the surface treatment, and the results point to incomplete debonding.

The stress–strain curve of filled material consisting of a matrix defined by eq. (8) and undergoing the debonding process [eqs. (10) and (14)] can be calculated and compared to experimental stress–strain curves. Optimized values of *K* and *B* are listed in Table III for polypropylene and in Table IV for polyamide 6. The value of the constant *K* decreases with the filler volume fraction for all four cases considered (polypropylene and polyamide 6 each filled with treated and untreated beads); in fact, it is nearly inversely pro-

portional to the filler volume fraction ϕ . On the other hand, the exponential term constant *B* increases with the filler concentration. The evolution of *K* and *B* constants with the filler volume fraction is consistent with the debonding occurring over a narrow effective stress $\bar{\sigma}$ range in the more highly filled composites. The agreement between the experimental stress–strain curves and those computed using the procedure described in this article is quite good (Fig. 10 for polypropylene, $\phi = 0.2$ and Fig. 11 for polyamide 6, $\phi = 0.25$). It confirms that the Bartenev equation can be used to describe the debonding process not only when the matrix is elastic¹⁷ but also when the composite nonelasticity is caused by a combination of the debonding and of the matrix viscoelasticity. Moreover, the Bartenev equation appears to be able to cover the cases of both complete and partial debonding (polypropylene and polyamide 6, respectively). When the calculated results are expressed in the form of the E_{sc}/E_{sm} ratio, an equally acceptable agreement with the experimental results is obtained (Fig. 12).

The debonding model can also be used to predict the stress–strain behavior of filled polymer at a different strain rate. This is shown in Figure 13, where the stress–strain curves of neat polypropylene (experimental and modeled using constants of Table I) and of filled polypropylene using the values of $K = 4.3 \cdot 10^{-2} \text{ MPa}^{-1} \text{ s}^{-1}$, and of *B*

Table IV *K* and *B* Values of Polyamide 6 (PA6)/Glass Beads Composites

Glass Content (vol. %)	$K \times 10^2 \text{ MPa}^{-1} \text{ s}^{-1}$		$B \times 10^2 \text{ MPa}^{-1}$	
	NT	T	NT	T
5	9.60	8.0	0.52	0.085
25	1.80	1.40	6.5	0.28
40	1.0	0.80	11.0	0.88

NT, untreated glass beads; T, silane-treated glass beads.

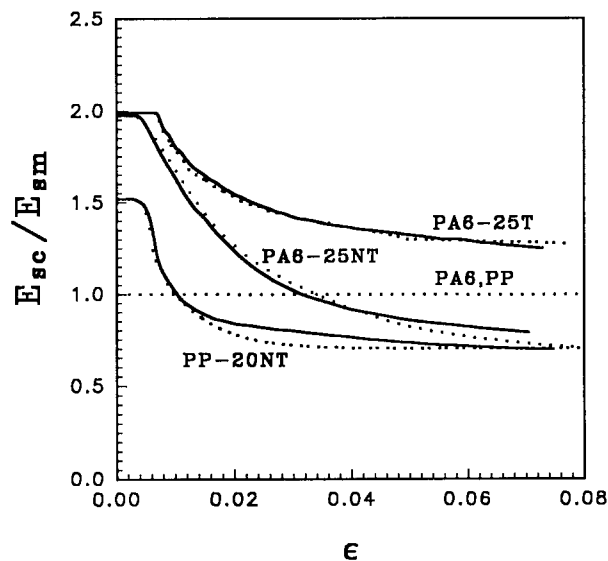


Figure 12 Calculated (\cdots) and experimental ($—$) E_{sc}/E_{sm} versus ϵ curves of 20 vol % filled PP and 25 vol % filled PA6.

$= 0.11 \cdot 10^{-2} \text{ MPa}^{-1}$ determined at $\dot{\epsilon} = 0.122 \cdot 10^{-2}$ but used to calculate the stress strain curves of the composite at $\dot{\epsilon} = 0.5 \cdot 10^{-2}$. The strain rate effect is particularly pronounced at high strain because, unlike yield stress, the initial modulus does not change. The applicability of the model to

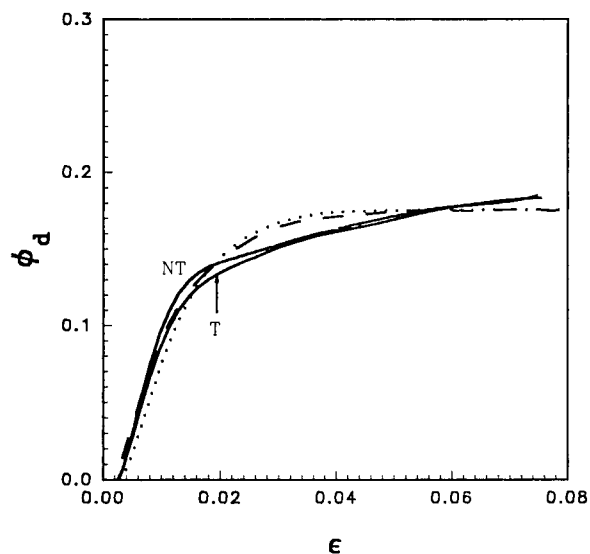


Figure 14 Debonded filler fraction, ϕ_d , as a function of strain, ϵ , calculated from experimental σ versus ϵ data using eq. (11) and those predicted by the model (NT \cdots , T $—$) for filled PP ($\phi = 0.2$).

evaluate the debonding process at different strain rates should be the subject of further studies.

The volume strain due to debonding ζ_d can be calculated with the help of eq. (19) and using ϕ_d versus ϵ function (Figs. 14 and 15) obtained either

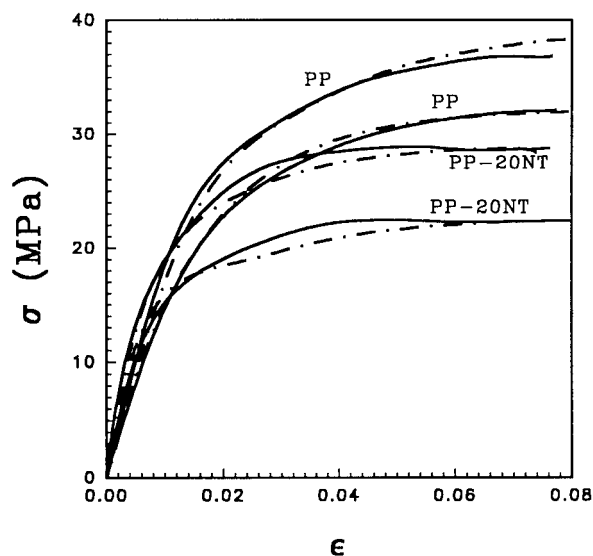


Figure 13 Experimental ($—$) and calculated (\cdots) stress-strain curve of neat polypropylene and filled polypropylene ($\phi = 0.2$). Effect of strain rate (a) $\dot{\epsilon} = 0.12\% \text{ s}^{-1}$ and (b) $\dot{\epsilon} = 0.5\% \text{ s}^{-1}$.

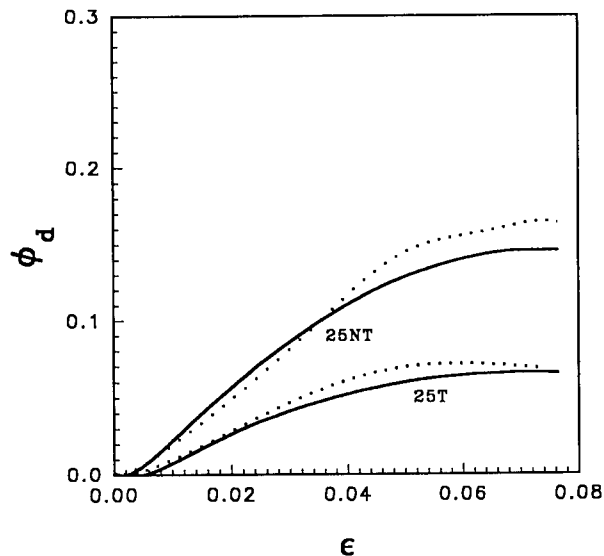


Figure 15 Debonded filler fraction, ϕ_d , as a function of strain, ϵ , calculated from experimental σ versus ϵ data using eq. (13) and those predicted by the model (\cdots) for filled PA6 ($\phi = 0.25$) treated (T) and untreated (NT).

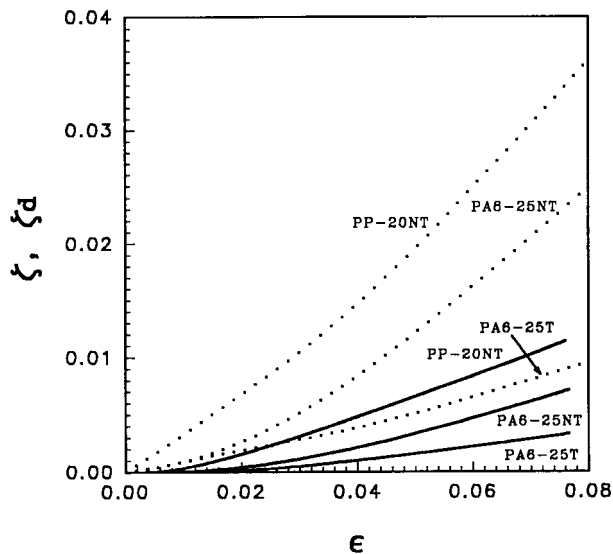


Figure 16 Total volume strain ζ (experimental) and debonded volume ζ_d calculated using eq. (18) as a function of strain-filled PP (NT) and filled PA6 (T and NT).

from the experimental data and eq. (10) or from the model. The results are very similar. The calculated ζ_d versus ϵ curves can be compared to the total volume strain recorded during the test (ζ vs. ϵ), as shown in Figure 16. The comparison suggests that in the range of strains where the debonding is initiated and where the rate of debonding is highest (e.g., for polypropylene, $\phi = 0.2$, at $0.4\% \leq \epsilon \leq 1.5\%$) the volume strain due to debonding is only a small part of the total volume strain and, due to the experimental error, would be difficult to extract from the experimental ζ versus ϵ curves.

CONCLUSION

The stress–strain behavior of two viscoelastic polymers, polypropylene and polyamide 6, filled with glass beads undergoing a constant strain rate test can be described by a model that takes into account the matrix viscoelasticity and that uses the Bartenev equation for the time dependence of the filler matrix interfacial strength. Depending on the level of filler matrix adhesion, complete or partial debonding is recorded in the strain range considered. The model can accommodate both situations.

NOMENCLATURE

A_1	constant, Kerner–Lewis [eq. (11)]
a, b, c, d	constants [eq. (8)]
B	debonding rate constant [eq. (14)]
B_1, B_2	constants, Kerner–Lewis equation [eqs. (11) and (12)]
D	damage parameter [eq. (1)]
D_m	Constant [eq. (7)]
d	filler particle diameter
\bar{E}	modulus of damaged material [eq. (1)]
E_{0c}, E_{0m}	initial modulus of composite and of matrix
E_1, E_2	relative moduli of the filled and of the fully debonded composite [eq. (11) and (12)]
E_{sc}, E_{sm}	secant moduli of composite and of matrix
E'_c	value of composite modulus used to calculate effective stress $\bar{\sigma}$ [eq. (15)]
Ψ	crowding factor
K	debonding rate constant [eq. (14)]
t	time (independent variable)
t_f	time of failure [eq. (13)]
t_r	relaxation time [eq. (4)]
ϵ	axial strain
ϵ_d	strain at which particles become debonded
ϵ_0	strain at which debonding starts
$\dot{\epsilon}$	strain rate
$\dot{\epsilon}_e, \dot{\epsilon}_n$	elastic and inelastic strain rate
ϕ, ϕ_b, ϕ_d	filler volume fraction, overall (ϕ), bonded (ϕ_b), and debonded (ϕ_d)
σ	nominal stress
$\dot{\sigma}$	rate of stress change
$\bar{\sigma}$	effective stress
ζ	total volume strain
ζ_d	volume strain due to debonding

REFERENCES

1. A. Meddad and B. Fisa, *J. Appl. Polym. Sci.*, to appear.
2. J. Lemaître and J. L. Chaboche, *Mécanique des Matériaux Solides*, 2nd ed., Dunod, Paris, 1988.
3. G. M. Newaz and W. J. Walsh, *J. Compos. Mater.*, **23**, 326 (1989).
4. L. L. Anderson and R. J. Farris, *Polym. Eng. Sci.*, **33**, 1458 (1993).
5. L. L. Anderson and R. J. Farris, *Polym. Eng. Sci.*, **33**, 1466 (1993).

6. F. C. Wong and A. Ait-kadi, *J. Appl. Polym. Sci.*, **55**, 263 (1995).
7. Yu. P. Zezin, *Mech. Compos. Mater.*, **30**, 131 (1994).
8. Y. H. Zhao and G. J. Weng, *Int. J. Damage Mech.*, **4**, 196 (1995).
9. G. Ravichandran and C. T. Liu, *Int. J. Solids Struct.*, **32**, 979 (1995).
10. G. Menges and E. Schmactenberg, *Kunstst.-Ger. Plast.*, **77**, 20 (1987).
11. L. E. Nielsen and R. F. Landel, *Mechanical Properties of Polymers and Composites*, 2nd ed., Marcel Dekker Inc., New York, 1994.
12. J. Jancar and A. T. DiBenedetto, *J. Mater. Sci.*, **29**, 4651 (1994).
13. I. Collias and D. G. Baird, *Polym. Eng. Sci.*, **35**, 1167 (1995).
14. M. M. Bartenev and Yu. S. Zuyev, *Strength and Failure of Viscoelastic Materials*, 1st ed., Pergamon Press, London, 1968.
15. I. I. Perepechko, *An Introduction to Polymer Physics*, 1st ed., Mir Publishers, Moscow, 1981.
16. R. J. Crawford, *Plastic Engineering*, 2nd ed., Pergamon Press, London, 1987.
17. A. Meddad and B. Fisa, *J. Mater. Sci.*, to appear.